Valence determination of rare earth elements in lanthanide silicates by L_3-XANES spectroscopy

Antonina N Kravtsova[1], Alexander A Guda[1], Joerg Goettlicher[2], Alexander V Soldatov[1], Vladimir K Taroev[3], Anvar A Kashaev[4], Lyudmila F Suvorova[3], Vladimir L Tauson[3]

[1] International Research Center "Smart materials", Southern Federal University, 5 Sorge Street, Rostov-on-Don 344090, Russia

[2] Karlsruhe Institute of Technology, ANKA Synchrotron Radiation Facility, Karlsruhe, Germany

[3] Vinogradov Institute of Geochemistry, Siberian Branch of R.A.S., Irkutsk, Russia

[4] Institute of the Earth's Crust, Siberian Branch of R.A.S., Irkutsk, Russia,

E-mail: akravtsova@sfedu.ru

Abstract. Lanthanide silicates have been hydrothermally synthesized using Cu and Ni containers. Chemical formulae of the synthesized compounds correspond to $K_3Eu[Si_6O_{15}]\cdot 2H_2O$, $HK_6Eu[Si_{10}O_{25}]$, $K_7Sm_3[Si_{12}O_{32}]$, $K_2Sm[AlSi_4O_{12}]\cdot 0.375H_2O$, $K_4Yb_2[Si_8O_{21}]$, $K_4Ce_2[Al_2Si_8O_{24}]$. The oxidation state of lanthanides (Eu, Ce, Tb, Sm, Yb) in these silicates has been determined using XANES spectroscopy at the Eu, Ce, Tb, Sm, Yb, L_3-edges. The experimental XANES spectra were recorded using the synchrotron radiation source ANKA (Karlsruhe Institute of Technology) and the X-ray laboratory spectrometer Rigaku R-XAS. By comparing the absorption edge energies and white line intensities of the silicates with the ones of reference spectra the oxidation state of lanthanides Eu, Ce, Tb, Sm, Yb has been found to be equal to +3 in all investigated silicates except of the Ce-containing silicate from the run in Cu container where the cerium oxidation state ranges from +3 (Ce in silicate apatite and in a KCe silicate with $Si_{12}O_{32}$ layers) to +4 (starting CeO_2 or oxidized Ce_2O_3).

1. Introduction

Synthesis and investigation of new silicates containing rare earth elements (REE) are of particular interest as they have a potential to determine the environmental conditions of mineral formation. From geochemical point of view such silicates may have significance as indicators of hydrothermal conditions of rare earth mineralization. REE-bearing silicates are also multi-functional group of novel compounds with increasing application areas. They have potential in photoluminescence, ion-exchange properties and electronics.

In the present investigation the synthesis of single crystals (up to 3 mm length) of REE-containing (REE = Eu, Ce, Tb, Sm, Yb) silicates were done under controlled conditions of formation [1-3]. Analysis of the chemical compositions and chemical structures of most of the synthesized silicates has already been performed [1-3].

In the paper we present the determination of the oxidation state of rare earth elements in the synthesized silicates on the basis of X-ray absorption near-edge structure (XANES) spectroscopy. XANES spectroscopy [4] is an effective method which allows obtaining information on electronic and local atomic structure around the absorbing type of atoms in materials in condensed state even without long-range order in atomic distribution [5]. In our research the oxidation state of lanthanides (Eu, Ce,

Content from this work may be used under the terms of the Creative Commons Attribution 3.0 licence. Any further distribution of this work must maintain attribution to the author(s) and the title of the work, journal citation and DOI.
Published under licence by IOP Publishing Ltd

Tb, Sm, Yb) was determined by comparing the absorption edge energies and white line intensities of the L_3-edge XANES spectra of the studied silicates (with an unknown oxidation state of the lanthanides) and reference samples (with well known lanthanide oxidation state). This technique was shown to be very effective for the oxidation state of ions determination in complex solids [6]. These data coupled with the crystal structures characteristics may be useful for diagnostics of mineral formation processes.

2. Experimental

Lanthanide (Eu, Ce, Tb, Sm, Yb) containing phases have been hydrothermally synthesized in the Vinogradov Institute of Geochemistry (Irkutsk, Russia). Synthesis of Eu, Ce, Sm, Yb-containing silicates was performed in Ni containers where oxygen fugacity (fO_2) was controlled by buffer association Ni-NiO (nickel-bunsenite, NB). For comparison Tb, Ce-containing silicates were synthesized in Cu containers where oxygen fugacity is controlled by a Cu-Cu_2O buffer. Experimental temperature was 500 ± 5 °C, the pressure in autoclaves was about 100 MPa. The duration of hydrothermal synthesis was 45 days. For Ce silicate synthesis in Cu-container three runs with differences in starting materials and in one case without Cu_2O have been performed (Table 1). Chemical formulae of the compounds synthesized in Ni containers correspond to $K_3Eu[Si_6O_{15}] \cdot 2H_2O$, $HK_6Eu[Si_{10}O_{25}]$, $K_7Sm_3[Si_{12}O_{32}]$, $K_2Sm[AlSi_4O_{12}] \cdot 0.375H_2O$, $K_4Yb_2[Si_8O_{21}]$, $K_4Ce_2[Al_2Si_8O_{24}]$. Electron microprobe analyses of the Ce run products from syntheses in Cu-container have not yet been carried out but powder synchrotron X-ray diffraction (XRD) gives first information about formed crystal phases.

Table 1. Experimental conditions for the three Ce silicate syntheses in Cu containers.

Experiment	Starting solution KOH [wt. %]	SiO_2 [g]	Al_2O_3 [g]	Cu_2O [g]	Ce-oxide [g]	CeF_3 [g]	Buffer after run
Ce-Cu1	15.25	12.48	1.90	5.0	1.0 (CeO_2)	--	Cu, Cu_2O
Ce-Cu2	15.25	9.61	1.6	5.5	8.0 (Ce_2O_3)	--	Cu only
Ce-Cu3	15.25	9.61	1,.6	−	8.02 (Ce_2O_3)	0.5	Cu only

L_3-XANES spectroscopy at the SUL-X beamline of the synchrotron radiation source ANKA (Karlsruhe Institute of Technology (KIT)) has been applied to obtain valence state of Ce and Tb in the run products from REE (aluminium) silicate syntheses. The SUL-X beamline uses a wiggler as radiation source. A Si(111) crystal pair installed in a fixed exit double crystal monochromator provided the monochromatic radiation. ANKA was operating at 2.5 GeV electron energy at electron current of 100 – 150 mA. X-ray energy was calibrated for the Ce L_3-edge with a Cr and for Tb L_3-edge with a Co metal foil to 5989 eV and 7009 eV, respectively (first inflection point). Calibration spectra were measured simultaneously with the sample spectra. Spot size at sample positon was about 0.8 mm x 0.8 mm (KB mirrors collimated). For small aggregates the beam has been focused to about 0.15 mm (hor.) x 0.1 mm (vert.) at the sample position.

Ce containing silicates have been selected as single crystals from the run in Ni container ($K_4Ce_2[Al_2Si_8O_{24}]$) [2] and as single crystals and polycrystalline aggregates from the runs in Cu containers. Samples were pressed to pellets when sufficient material could be selected or fixed on Kapton tape and measured in transmission using ionization chambers as detectors and at the same time in fluorescence mode (beam – sample – detector angles: each 45°) with a 7 element Si(Li) solid state detector (SGX Sensortech, former Gresham). Transmission data were preferred when concentrations of the absorbing element were high like for Ce sample in Ni-container and the Tb sample, whereas for some Ce containing single crystals and polycrystalline aggregates of the run in Cu-containers fluorescence data gave better signal to noise ratio. Gas fillings of the first, second and third ionization

chamber were - for the Ce L_3-edge 600 mbar N_2, 370 and 630 mbar Ar20%N80%, and for the Tb L_3-edge 200 and 630 mbar Ar20%N80% and 266 mbar Ar. For measurements in fluorescence mode Ce and Tb $L\alpha$ emission intensities have been recorded between 4440 and 5160 eV, and 5910 and 6550 eV, respectively. Pre-edge background have been measured 150 eV before the edge with 5 and 2 eV energy step widths, across the edge (-20 to +20 eV) with 0.3 eV step width (all counting times 1s per step) and above the edge up to k 10.8 for Ce and 13.9 for Tb with square root of k as counting time. Edge energies for Ce L_3 and Tb L_3 were set to 5.723 and 7.514 keV, respectively. Pre-edge, post-edge corrections and edge jump normalization have been performed with the ATHENA code [7]. Data quality of the spectra was not sufficient for EXAFS analysis because focus was put on screening the XANES region of many aggregates. Hence, measurement parameters were optimized for fast data accumulation giving sufficient signal to noise ratio just in the XANES region. Moreover, EXAFS data evaluation is not possible in the cases of polycrystalline aggregates that consist of at least two Ce containing phases, and is difficult in the cases where measurements had to be done on single crystals directly due to orientation effects because sufficient material was not available for grinding and preparing pellets.

Eu L_3-, Ce L_3-, Sm L_3-, Yb L_3-XANES spectra of investigated silicates and reference samples were also recorded using X-ray absorption laboratory spectrometer Rigaku R-XAS. XANES spectra were measured in the transmission mode. A tungsten cathode and a Ge (311) crystal monochromator were used. X-ray tube voltage was 20 kV and current was 70 mA. A gas-filled proportional counter (argon gas at a pressure of 300 mbar) was used to register the intensity of the incident radiation, while a scintillation detector was used to register transmitted radiation.

Additionally, powder synchrotron X-ray diffraction (XRD) at the SUL-X beamline (Si(111) crystal pair as monochromator) was used to identify crystal phases from the Ce silicate syntheses in Cu containers where electron microprobe analysis have not yet been carried out. A CCD detector (XDR VHR-2 150, Photonic Science) have been used in symmetric transmission geometry in 16 bit fusion mode with 2 x 2 binning with a beam focused to about 150 µm (hor.) x 100 µm (vert.) at the sample position. Lattice plane distances have been calibrated with LaB_6 (NIST 660b), and CCD diffraction images were radially integrated to 1D XRD pattern using the Fit2D software [8]. With the given energy (17 keV, about 0.73 Å) and sample detector distance (about 106 mm) the lower limit of d-values range down to about 1.2 Å. The upper limit of d values was about 15 Å due to the primary beam stop. Further data evaluation for crystal phase identification has been performed with the DIFFRAC.EVA software (V 4.1.1, Bruker) [9] and the ICDD powder diffraction database.

3. Results and discussion

The positions of the white line of the Ce L_3 spectrum of the single crystals from the runs in Ni and Cu containers are close to the white line position of the $Ce(III)(NO_3)_3$ reference spectrum whereas the polycrystalline aggregates from the runs in Cu containers contain Ce(IV) besides Ce(III) in different fractions, even in the runs with Ce_2O_3 and CeF_3 as starting material (Figure 1b,c). Single crystals in general show only Ce(III). Ce(IV) in the fine and coarse grained material represent unreacted or dissolved and re-precipitated $Ce(IV)O_2$ verified by XRD for the run Ce-Cu1 or is due to oxidized Ce_2O_3 starting material for the runs Ce-Cu2 and Ce-Cu3 (Table 1, Figure 1b,c,d). Ce(III) in the fine and coarse grained material as well as in single crystals (Figure 1b,c) are most probably incorporated into silicate structures.

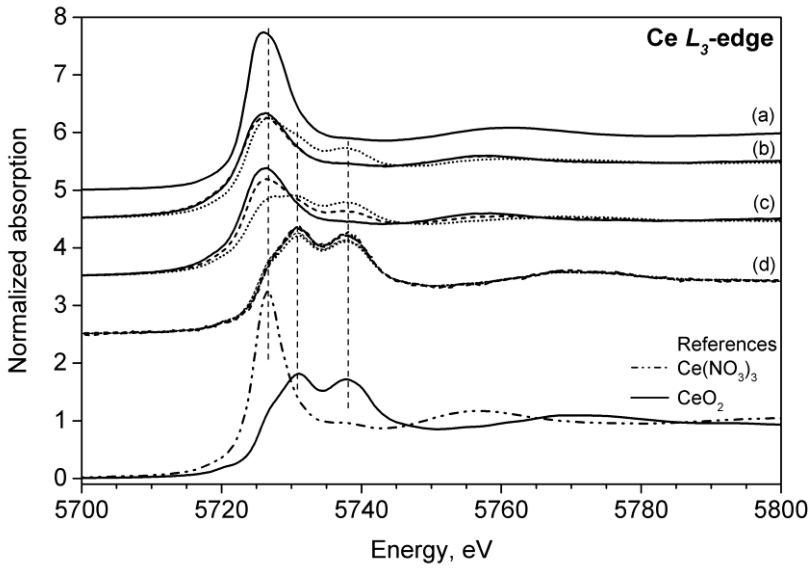

Figure 1. Ce L_3-XANES spectra of run products from synthesis in Ni-container ($K_4Ce_2[Al_2Si_8O_{24}$ (a)) and from runs in Cu-containers Ce-Cu3 (b), Ce-Cu2 (c), and Ce-Cu1 (d). Spectra of single crystals (solid lines), of coarse polycrystalline (dashed lines) and fine polycrystalline aggregates (dotted lines) are compared with $Ce(III)(NO_3)_3$ (dash-double dotted line) and $Ce(IV)O_2$ (solid line) reference spectra.

XRD confirms CeO_2 for the sample fractions where Ce(IV) has been detected in the Ce L_3-XANES spectra (Figure 2). Other Bragg reflexions matches with KAl feldspar ($KAlSi_3O_8$, most probably as the Al, Si disordered sanidine phase), and sometimes with $KAlSiO_4$ (kalsilite). The latter is not shown here. The remaining patterns of the Bragg peaks of the run products from Cu containers (Ce-Cu2, Ce-Cu3) are very similar to $Ce_{9.33}(SiO_4)_6O_2$ which has apatite structure [10]. Due to the presence of K during synthesis also a silicate apatite with $KCe_9(SiO_4)_6O_2$ composition analogous to $KPr_9(SiO_4)_6O_2$ [11] is under discussion, and has to be verified by electron microprobe analysis. A KCe silicate apatite has not been described so far. Ce is 3+ in the apatite structure which is confirmed also by the Ce(III) whiteline increases in the Ce L_3-XANES spectra of the sample fractions were Bragg reflexion of the silicate apatite are intense and reflexions of the CeO_2 are low in the X-ray diffractograms (Figure 2). The apatite structure is also supported by the hexagonal habitus of some of the single crystals detected in the run products. Single crystal structure investigation has been started for verification. $KPr_9(SiO_4)_6O_2$ is mentioned as a potential oxide ion conductor [11]. Recently silicate apatites have been synthesized with Na, Ca and Eu, Gd, Sm, and also K and Pr [12], and Li and Eu, Ce, Tb [13]. Such compounds are discussed as new optical materials, e.g., as phosphors for application in solid-state lighting. Our investigations show that REE silicate apatites can also form under hydrothermal conditions (500 °C, 1 kbar) apart from the solid state and flux procedures described in [12,13].

The XRD of one aggregate of the Ce-Cu2 run is similar to the pattern of $K_8Nd_3(Si_{12}O_{32})(OH)$ (ICDD, pdf No. 49-53 orr 80-2178) (Figure 3). Such type of K-REE silicates with $Si_{12}O_{32}$ layers have recently been described also for K-Sm and K-Tb silicates ($K_{7.814}Sm_3Si_{12}O_{32}(OH)_{0.814} \cdot 0.77H_2O$, $K_{7.04}Tb_3Si_{12}O_{32.02} \cdot 1.36H_2O$) [14]. The new compound has probably the composition $K_7Ce_3(Si_{12}O_{32}) \cdot nH_2O$ [this study, and personal communication, Sergey Aksenov]. The corresponding Ce L_3-XANES spectrum of the polycrystalline aggregate shows some Ce(IV) because CeO_2 is present besides the KCe silicate with $Si_{12}O_{32}$ layers where Ce is +3 (Figure 3).

Only Ce(IV) have been found in the run Cu-Cu1 (Figure 1d) where few large fragments do not show crystal faces and are gel like amorphous products. XRD of the aggregates that are the main fraction in this run shows CeO_2 and a KAl feldspar ($KAlSi_3O_8$). This run was the only one in Cu-containers with CeO_2 as starting material and where Cu_2O added as buffer was still present after the run. High oxygen fugacity may have prevented Ce(IV) from reduction and hence from incorporation into silicates, and just $KAlSi_3O_8$ feldspar had formed.

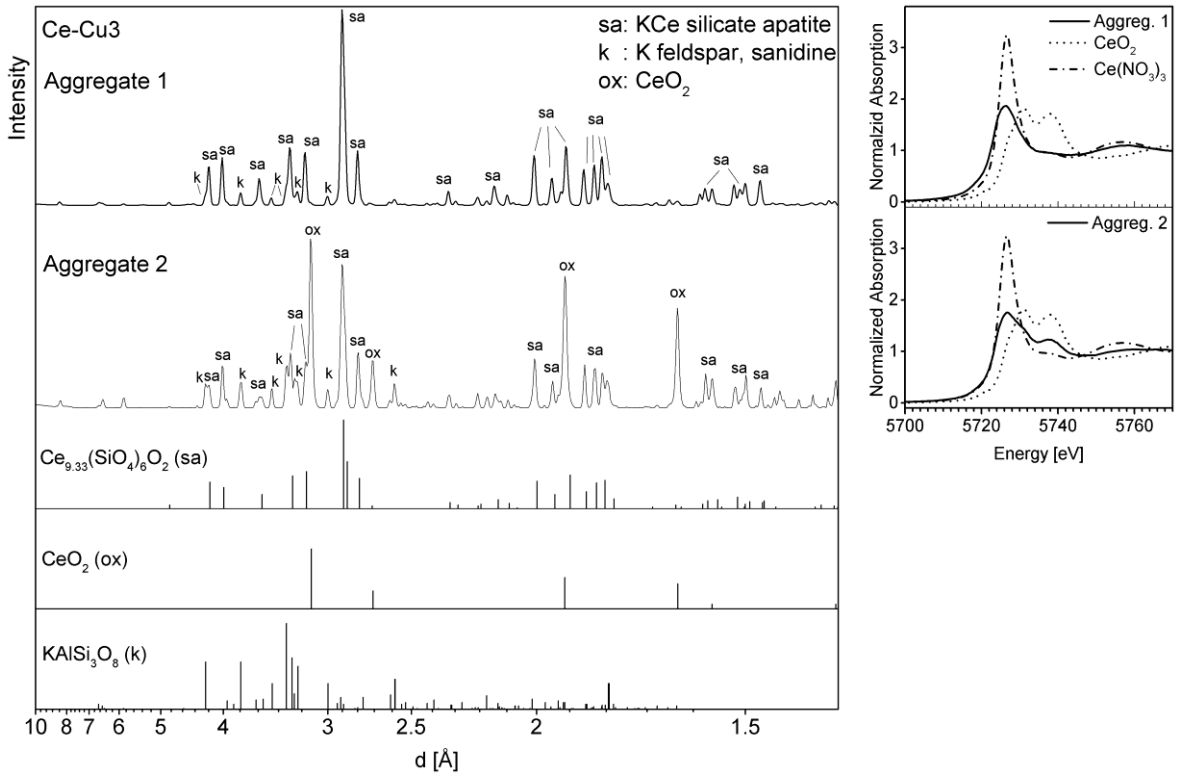

Figure 2. Powder synchrotron X-ray diffractograms and Ce L_3-XANES spectra of products from Ce silicate synthesis in Cu container (Ce-Cu3) resulting in CeO_2, K-feldspar and a Ce or KCe silicate apatite and Ce(IV) and Ce(III) fractions for polycrystalline aggregate 2; and K-feldspar and (K)Ce silicate apatite and only Ce(III) for aggregate 1. For the latter, the absence of Ce(IV) in the XANES data is in agreement with the absence of CeO_2 in the XRD and proves that Ce is +3 in the (K)Ce silicate apatite. Reference line patterns for XRD are $Ce_{9.33}(SiO_4)_6O_2$ (ICDD pdf No. 43-443), CeO_2 (34-394)and $KAlSi_3O_8$ (sanidine) (25-618); and for the Ce L_3-XANES spectroscopy CeO_2 and $Ce(NO_3)_3$ are references for Ce(IV) and Ce(III), respectively.

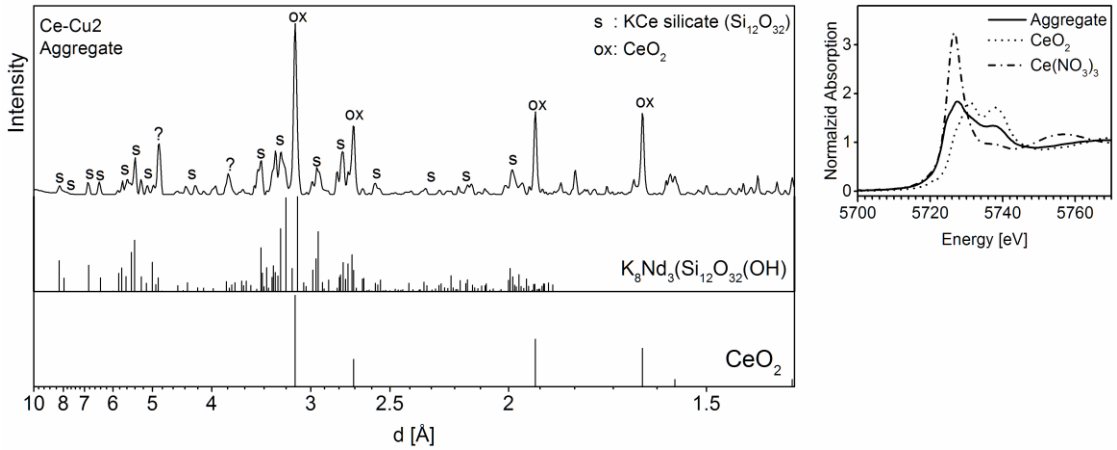

Figure 3. Powder synchrotron X-ray diffractogram and corresponding Ce L_3-XANES spectrum of an aggregate from Ce silicate synthesis in Cu container (Ce-Cu2). The X-ray diffractogram shows CeO_2 and a pattern similar to the one of $K_8Nd(Si_{12}O_{32})OH$ (ICDD, pdf No. 49-53 or 80-2178, here 80-2178). The Ce L_3-XANES spectrum confirms the Ce $^{4+}$ of CeO_2. From Ce L_3-XANES analysis and the structure of such silicates Ce is assumed to be 3+.

Tb ion oxidation state has been determined to be equal to +3 because the white line of the spectrum of the Tb polycrystalline aggregates from the run in Cu-container is close to the lower energy position of the two white lines of a Tb(III,IV) mixed oxide (Figure 4; [15]). This is a similar result as for Ce in some of the coarse aggregates and single crystals from runs Ce-Cu2 and Ce-Cu3 (Figure 1b,c). The Tb silicate has already been determined to $K_7Tb_3Si_{12}O_{32} \cdot 1.35\ H_2O$ in [14].

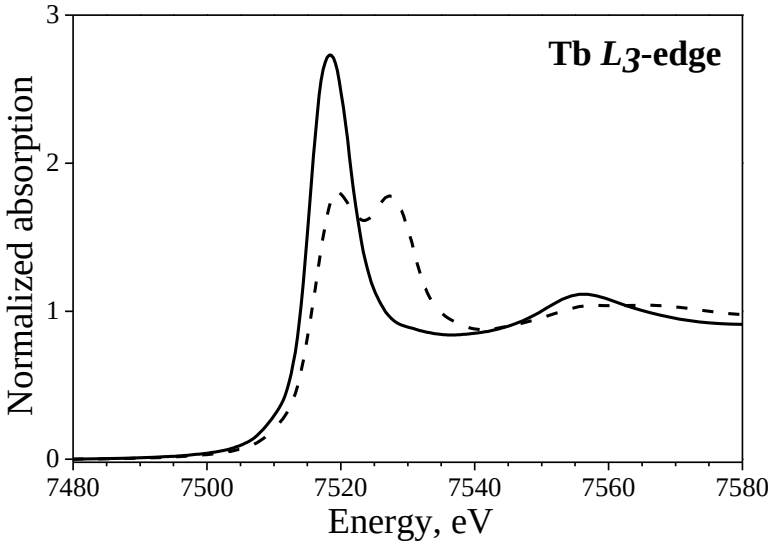

Figure 4. Tb L_3-XANES spectra: Run product from synthesis in Cu-container ($K_7Tb_3Si_{12}O_{32} \cdot 1.35\ H_2O$) [14] (solid line), TbO_x (x=1.5-2) reference (dashed line).

In Figure 5 we present a comparison of the experimental Eu L_3-XANES spectra of $K_3Eu[Si_6O_{15}] \cdot \cdot 2H_2O$, $HK_6Eu[Si_{10}O_{25}]$ and the ones of reference substances, $Eu^{2+}S$ with oxidation state +2 and $Eu^{3+}F_3$, $Eu^{3+}{}_2O_3$ with oxidation state +3. It can be seen that the energy of the main maximum of Eu L_3-XANES spectra is ~6983.2 eV for EuF_3, Eu_2O_3 (Eu oxidation state is +3) and ~6975.2 for EuS (Eu oxidation state is +2). The main maximum energies of Eu L_3-XANES spectra of $K_3Eu[Si_6O_{15}] \cdot 2H_2O$ and $HK_6Eu[Si_{10}O_{25}]$ silicates are consistent with the main maximum energy of the $Eu^{3+}{}_2O_3$. So, it is possible to conclude that Eu in the $K_3Eu[Si_6O_{15}] \cdot 2H_2O$, $HK_6Eu[Si_{10}O_{25}]$ synthesized silicates has the oxidation state +3.

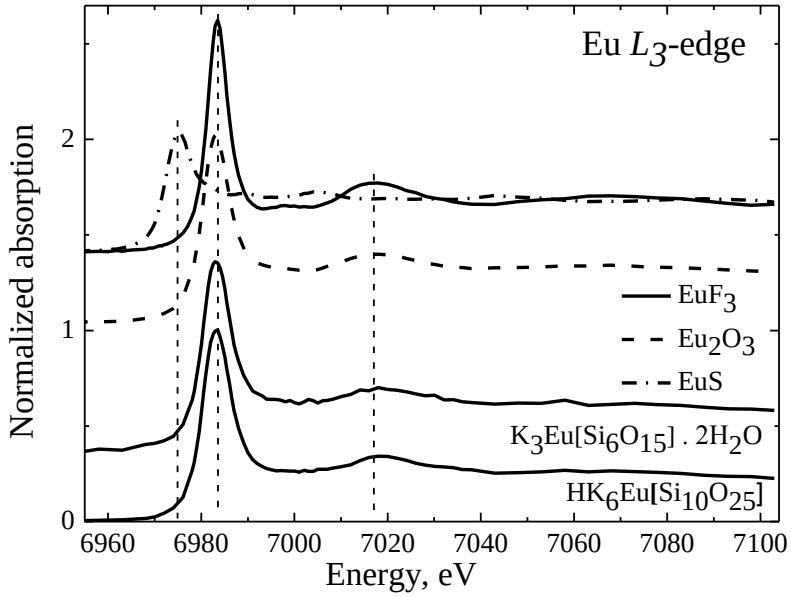

Figure 5. Comparison of the experimental Eu L_3-XANES spectra of $K_3Eu[Si_6O_{15}] \cdot 2H_2O$, $HK_6Eu[Si_{10}O_{25}]$ silicates and $Eu^{3+}F_3$ (upper solid line), $Eu^{3+}{}_2O_3$ (dashed line), $Eu^{2+}S$ (dash-dotted line) reference spectra.

On the basis of the analysis of the edge energies of the Sm L_3-, Yb L_3-XANES spectra it was found that the oxidation state of Sm and Yb in $K_7Sm^{3+}{}_3[Si_{12}O_{32}]$, $K_2Sm^{3+}[AlSi_4O_{12}] \cdot 0.375H_2O$, $K_4Yb^{3+}{}_2[Si_8O_{21}]$ silicates is equal to 3+ [16].

4 Conclusions

The oxidation state of rare-earth elements (REE=Eu, Ce, Tb, Sm, Yb) in new synthesized REE-containing silicates has been determined using XANES spectroscopy near REE L_3-edges. Comparison of the absorption edge energies of the silicates with the ones of reference substances allowed to determine the oxidation state of Eu, Ce, Tb, Sm, Yb in all investigated silicates equal to +3 except for the Ce-containing silicate synthesized in Cu containers where Ce was found also in oxidation state +4 most probably due to non-reacted CeO_2 or oxidized Ce_2O_3 starting material that has not been incorporated into silicates. A Ce or KCe silicate apatite has been discovered from two runs in Cu-containers.

We are incredibly sad to report that Vladimir Taroev died suddenly on January 28, 2016. He was an experimental mineralogist and petrologist by heart with his specialty of hydrothermal synthesis of feldspars and new REE silicates.

Acknowledgments

The work is supported by the grant of the Russian Foundation for Basic Research No. 14-05-00580 and No. 16-05-00392.

References

[1] Aksenov S M, Rastsvetaeva R K, Rassylov V A, Bolotina N B, Taroev V K and Tauson V L (2013) *Micropor. Mesopor. Mater.* **182** 95-110
[2] Aksenov S M, Rassylov V A, Rastsvetaeva R K and Taroev V K (2013) *Crystallography Reports* **58**, N 6 835-41
[3] Rastsvetaeva R K, Aksenov S M and Taroev V K (2010) *Crystallography Reports* **55**, 6 1041-49
[4] Bunker G 2010 *Introduction to XAFS. A Practical Guide to X-ray Absorption Fine Structure Spectroscopy* (Cambridge University Press)
[5] Mansour A N, A. Marcelli A, Cibin G, G. Yalovega G, Sevastyanova T and Soldatov A V (2002) *Phys Rev B* **65** 134207
[6] Vitova T, K. Kvashnina K O, Nocton G, Sukharina G, Denecke M A, Butorin S M, Mazzanti M, Caciuffo R, Soldatov A, Behrends T and Geckeis H (2010) *Phys Rev B* **82** 235118
[7] Ravel B, Newville M (2005) *J. Synchrotron Rad.* **12** 537–41
[8] Hammersley A P, Svensson S O, Hanfland M, Fitch A N, Hausermann D (1996) *High Pressure Res.* **14**, 235-48
[9] BRUKER (2015): DIFFRAC.EVA. V 4.1.1 - https://www.bruker.com/products/x-ray-diffraction-and-elemental-analysis/x-ray-diffraction/xrd-software/eva/overview.html
[10] Belokoneva E L, Petrova T L, Simonov M A, Belov N V (1972) *Soviet physics, Crystallography* **17** 429-31
[11] Werner F, Kubel F. (2005) *Materials Letters*, **59**, 3660–5
[12] Latshaw A M, Hughey K D, Smith M D, Yeon J, zur Loye H-C (2015) *Inorg. Chem.* **54**(3) 876–84
[13] Kim D, Park D, Oh N, Kim J, Jeong E D, Kim S-J, Kim S, Park J-C (2015) *Inorg. Chem.* **54** 1325−36
[14] Taroev V K, Kashaev A A, Malcherec T, Goettlicher J, Kaneva E V, Vasiljev A D, Suvorova L F, Suvorova D S and Tauson V L (2015) *Solid State Chemistry* **227** 196-203
[15] Potdevin A, Chadeyron G, Briois V, Leroux F and Mahiou R (2010) *Dalton Trans.* **39** 8718–24
[16] Kravtsova A N, Guda A A, Soldatov A V, Goettlicher J, Taroev V K, Kashaev A A, Suvorova L F and Tauson V L (2015) *Optics and Spectroscopy* **119**, N 6 982-86